Transport in Porous Media (2006) 65: 213–236
DOI 10.1007/s11242-005-6081-8

Diffuse-interface Modeling of Two-phase Flow for a One-component Fluid in a Porous Medium*

P. PAPATZACOS** and S. M. SKJÆVELAND
University of Stavanger, Stavanger 4036, Norway

(Received: 26 January 2005; accepted in final form: 7 December 2005)

Abstract. The diffuse-interface (DI) model for the two-phase flow of a one-component fluid in a porous medium has been presented by Papatzacos [2002, *Transport Porous Media* **49**, 139–174] and by Papatzacos and Skjæveland [2004, *SPE J.* (March 2004), 47–56]. Its main characteristics are: (i) a unified treatment of two phases as manifestations of one fluid with a van der Waals type equation of state, (ii) the inclusion of wetting, and (iii) the absence of relative permeabilities. The present paper completes the presentation by including the implementation of wetting in the general case of a mixed-wet rock. As a result of this implementation, some statements are made about capillary pressure, confirming similar statements by Hassanizadeh and Gray [1993, *Water Resour. Res.* **29**, 3389–3405]. As an application of the model, we show that relative permeabilities depend on the spatial derivatives of the saturation.

Key words: diffuse-interface, two-phase flow, wetting.

1. Introduction

A new model for two-phase flow in porous media has recently been presented in two papers, referred to below as P1 (Papatzacos, 2002) and P2 (Papatzacos and Skjæveland, 2004). It is based, at the pore level, on the diffuse-interface (DI) model of a one-chemical-component fluid (see Anderson *et al.*, 1998; Papatzacos, 2000) characterized by (i) the two phases are manifestations of one and the same fluid, (ii) the transition from one phase to the other is taken care of by an additional term in the Navier–Stokes equation and by an equation of state of the van der Waals type, and (iii) the wetting properties are described by a boundary condition involving the normal gradient of the fluid density (the Cahn theory).

The upscaling from the pore level to the Darcy level is performed in P1, where the assumption of a constant and uniform temperature is also introduced. (We point out that that the assumption of constant temperature was

*This paper builds on results presented as SPE84546 at the 2003 SPE Annual Technical Conference and Exhibition, held October 5–8 in Denver.

**Author for correspondence: e-mail: paul.papatzacos@uis.no

introduced as a simplification – the energy-balance equation drops out – and is not a limitation inherent to the DI model.) A general method for the inclusion of wetting at the Darcy level is given in P1, but it is relatively complicated and its explicit implementation is not attempted in that paper. It is then shown in P2 that a considerable simplification can be obtained, for the implementation of wetting at the Darcy level, if one assumes that the wetting angles at the pore level are neither 0 nor 180°, but anywhere in between. The expression *incomplete wetting approximation* is used in P2 for this simplification. The explicit implementation of wetting is illustrated in P2, in the restricted case of a vapor wet rock. It is one of the purposes of this paper to generalize the implementation to a mixed wet rock. One then obtains a model which we shall call the *DI-model* in the sequel.

This model is presented in detail in Section 2 below. Its main characteristics are as follows. It concerns a one-chemical-component fluid capable of existing in two phases, which are conveniently referred to as the *liquid* and *vapor* phases. It has just one flow equation, in contradistinction to the traditional model of two-phase flow where each phase has its flow equation. This flow equation is a partial differential equation of the Cahn–Hilliard type. The traditional constants of permeability and porosity are input parameters, in addition to a constant Λ which is directly related to the thickness of the transition region. It is to be noted that the model does not use relative permeabilities. An equation of state of the van der Waals type is needed, and the wetting properties are deduced from the information contained in the traditional capillary pressure function.

The DI-model is thus ideally suited to the description of steam-water systems or similar, if the temperature gradients are negligible. But it can also be applied to oil–gas flows in situations where oil and gas can be described, thermodynamically and to an acceptable approximation, as the two phases of one and the same fluid.

Since the DI-model does not use relative permeabilities it should be possible to use it as a tool to test various hypotheses about these quantities. It must be pointed out, however, that such a use of the model is not straightforward, because its dependent variables (density, velocity, ...) characterize the *fluid* and there is no obvious method for finding *phase* quantities such as, say, vapor and liquid velocities. We give one possible method in P2, which satisfies some obvious physical criteria (conservation of momentum is one example); we then proceed to calculate relative permeabilities through their definitions in terms of phase velocities and pressure gradients, after having carried out numerical experiments. The calculations in P2 are restricted to a *stabilized* flow type (i.e., a flow type that can be described as a constant velocity traveling wave) and it is found there that the formulas defining relative permeabilities can be turned into analytic expressions. These give the relative permeabilities in terms of the equation of state, the

capillary pressure, and some parameters. See Section 3 below, where the expressions are generalized to the case of a mixed wet rock. (A two-phase saturated reservoir rock is often classified as having mixed wettability if each fluid wets part of the internal rock surface.)

Section 2 below presents the *DI-model*. Analytic expressions for the relative permeabilities of stabilized flows in a mixed wet porous medium are given in Section 3.

We return to the relative permeability concept in Section 4. Even if the concept is absent from the DI-model, it is certainly of interest to traditional two-phase flow, and therefore an important subject. We see it here as an interesting numerical application of the DI-model. In Section 4 we consider a one-dimensional mixed-wet porous medium, and use the DI-model to perform numerical experiments describing *non-stabilized* flow types, thus generalizing the investigation carried out in P2. We calculate "experimental" relative permeabilities and draw some conclusions.

2. Description of the DI-model

The DI-model is a Darcy level model of flow in a porous medium, of a fluid consisting of one chemical component. The rock matrix is assumed to be rigid, and the temperature is assumed uniform, constant, and subcritical.

The upscaling from the pore level to the Darcy level, is done in P1 by using the averaging technique of Marle (1982). It is shown in P2 that the assumption of incomplete wetting at the pore level results in just one flow equation at the Darcy level, the mass balance equation, involving one dependent variable, the upscaled fluid density. This we denote by R instead of the more traditional ρ, according to the notation introduced in P1 (and later used in P2), and following Marle's recipe of using capital letters for upscaled quantities.

The flow equation and the boundary conditions involving R are described in Section 2.1. The thermodynamics of the fluid, comprising the equation of state and the interaction energy due to wetting, is described in Section 2.3

2.1. FLOW EQUATION, INITIAL AND BOUNDARY CONDITIONS

The central equation of the DI-model is the Darcy level flow equation,

$$\frac{\partial R}{\partial t} = \nabla \cdot \left(\frac{K R^2}{\phi \eta} \nabla \left(\frac{d\Psi}{dR} - \Lambda \nabla^2 R + G \right) \right), \tag{1}$$

where K is the absolute permeability, ϕ the porosity, and Λ a constant related to the thickness of the transition region between the vapor and liquid phases (see P1); η is the fluid viscosity, Ψ is total Helmholtz free

energy per unit volume of bulk fluid (*bulk* being defined at the beginning of Section 2.3), and G is the gravitational potential causing an acceleration equal to $-\nabla G$. Functions Ψ and η depend on R alone, and the ways to determine them are given in Sections 2.3 and 2.2.

Note that Equation (1) is a mass balance equation, with a fluid velocity defined as

$$\mathbf{V} = -\frac{K R}{\phi \eta} \nabla \left(\frac{d\Psi}{dR} - \Lambda \nabla^2 R + G \right), \tag{2}$$

(It is shown in P1 that Equation (2) is the Darcy level momentum balance equation of the fluid, and that the traditional velocity results from setting $\Lambda = 0$.) Note also that Equation (1) is (when G is identically zero) a Cahn–Hilliard equation (see, for example, Novick–Cohen and Segel, 1984).

The boundary conditions of the model are usually written in terms of two quantities, u_1 and u_2, defined as follows:

$$u_1 = R, \tag{3a}$$

$$u_2 = \frac{d\Psi}{dR} - \Lambda \nabla^2 R + G. \tag{3b}$$

A well-posed problem for Equation (1) is obtained by supplying an initial condition $R(\mathbf{x}, 0) = F(\mathbf{x})$ (a given function of $\mathbf{x}$), and a boundary condition having one of the forms (a) to (e) below.

$$(a)\ H = 0, \quad (b) \begin{cases} u_1 = \alpha_1, \\ u_2 = \alpha_2, \end{cases} \quad (c) \begin{cases} \mathbf{n} \cdot \nabla u_2 = G_2 \\ u_2 = \alpha_2 \end{cases}, \tag{4a}$$

$$(d) \begin{cases} u_1 = \alpha_1 \\ \mathbf{n} \cdot \nabla u_1 = G_1 \end{cases}, \quad (e) \begin{cases} \mathbf{n} \cdot \nabla u_1 = G_1 \\ \mathbf{n} \cdot \nabla u_2 = G_2 \end{cases}. \tag{4b}$$

In these equations, $\mathbf{n}$ is the unit normal to the boundary, pointing out; H is a function of u_1 and u_2; α_1 and α_2 are two constants; and G_1 and G_2 are functions of $\mathbf{x}$, and of u_1 and u_2 and their derivatives.

A boundary condition on u_1 in the present model is equivalent, because of the equation of state, to a condition on the pressure in the traditional model. A boundary condition on $\mathbf{n} \cdot \nabla u_2$ is a condition on the velocity. The boundary conditions involving $\mathbf{n} \cdot \nabla u_1$ are new to this model and have been discussed in P1: they specify the angle between the isodensity lines and the reservoir surface. The boundary conditions which are relevant to reservoir studies are thus the ones labeled (d) and (e) above. For the special case of one-dimensional studies, as the ones presented in the present paper, it is natural to use $G_1 = 0$ (see P1).

2.2. THE FLUID VISCOSITY

Fluid viscosity must be known as a function of R in order to solve the flow equation (1). The formula for $\eta(R)$ that has been used in P1 and P2 is a modified form of a formula proposed by Arrhenius,

$$\eta = \eta_{\mathrm{l}}^{S_{\mathrm{l}}} \eta_{\mathrm{v}}^{S_{\mathrm{v}}}, \tag{5}$$

where η_{l} and η_{v} are the viscosities of the pure liquid and vapor phases, and S_{l} and S_{v} are the liquid and vapor saturations. In the present model, these are interpreted as follows:

$$S_{\mathrm{l}} = \frac{R - R_{\mathrm{v}}}{R_{\mathrm{l}} - R_{\mathrm{v}}}, \quad S_{\mathrm{v}} = \frac{R_{\mathrm{l}} - R}{R_{\mathrm{l}} - R_{\mathrm{v}}}. \tag{6}$$

2.3. THERMODYNAMICS

We now define the thermodynamics of the Darcy level fluid, and thereby determine the function $\Psi(R)$.

We remind the general assumptions. The temperature is uniform and constant. The fluid consists of one chemical component, and is capable of undergoing a phase transition so that two coexisting phases are possible. The phases are called *liquid* and *vapor*. There is a transition region of definite thickness between the phases, where the density gradients are large. We define *bulk fluid* to be the fluid which is far enough from the transition region that the density gradients are negligible and thus do not contribute to its free energy.

The bulk fluid has an equation of state of the van der Waals type.

It is shown in P2 that the total Helmholtz free energy per unit volume of bulk fluid consists of two parts and is written

$$\Psi(R) = \Psi^{\mathrm{b}}(R) + I(R). \tag{7}$$

The first part, Ψ^{b}, is the free energy per unit volume of bulk fluid. The equation of state can be expressed through it as follows:

$$P^{\mathrm{b}}(R) = R^2 \frac{d}{dR}\left(\frac{\Psi^{\mathrm{b}}}{R}\right), \tag{8}$$

where P^{b} is the pressure of bulk fluid. The determination of Ψ^{b} is given in Section 2.3.1.

The second part, I, is introduced in P1 for the description of wetting. An example of how I can be determined is given in P2. The general method is given in Section 2.3.2 below.

2.3.1. *The Equation of State and* Ψ^{b}

Let us consider a fluid of one chemical component, capable of existing in two phases with densities R_{v} and R_{l}, and where the chemical potential and the pressure at equilibrium are two constants denoted $\bar{M}$ and $\bar{P}$ respectively. Then it can be shown (see Appendix A in P1, and references given there) that the intrinsic Helmholtz free energy per unit volume of bulk fluid has the form

$$\Psi^{\mathrm{b}}(R) = W(R) + \bar{M}R - \bar{P}, \tag{9}$$

where $W(R)$ has the shape of a fourth order polynomial, with two minima of value zero occurring at two distinct values. (We shall in the sequel refer to such functions as being "W-like".) The minima of $W(R)$ are at $R = R_{\mathrm{v}}$ and $R = R_{\mathrm{l}}$.

It is shown in P1 that, when assuming uniform temperature as we do here, the value of $\bar{M}$ is irrelevant and one can set

$$\bar{M} = 0. \tag{10}$$

If quantitative results are expected from solving the well-posed problem outlined in Section 2.1, then it is important to obtain R_{v}, R_{l} and $W(R)$, at the specified temperature, from the relevant equation of state. Densities R_{v} and R_{l} are usually found by the Maxwell equal area rule. With an equation of state where bulk pressure P^{b} is given as a function of density R, this is

$$\int_{R_{\mathrm{v}}}^{R_{\mathrm{l}}} P^{\mathrm{b}}(R') \frac{dR'}{R'^2} = P^{\mathrm{b}}(R_{\mathrm{v}}) \left(\frac{1}{R_{\mathrm{v}}} - \frac{1}{R_{\mathrm{l}}} \right). \tag{11}$$

The $W(R)$-function is found by integrating Equation (8). As shown in P2, this leads to

$$W(R) = P^{\mathrm{b}}(R_{\mathrm{v}}) \left(1 - \frac{R}{R_{\mathrm{v}}} \right) + R \int_{R_{\mathrm{v}}}^{R} P^{\mathrm{b}}(R') \frac{dR'}{R'^2}. \tag{12}$$

Using the van der Waals equation of state as an example, i.e.,

$$P^{\mathrm{b}}_{\mathrm{v}dW}(R) = \frac{NkT\,R}{1 - BR} - AR^2 \tag{13}$$

(N is the number of molecules, k is Boltzmann's constant, T is the temperature, and A and B are two positive constants) we obtain for the van der Waals W-function,

$$W_{\mathrm{v}dW} = P^{\mathrm{b}}_{\mathrm{v}dW}(R_{\mathrm{v}}) \left(1 - \frac{R}{R_{\mathrm{v}}} \right) + AR(R_{\mathrm{v}} - R) + NkT\,R \ln \frac{R(1 - BR_{\mathrm{v}})}{R_{\mathrm{v}}(1 - BR)}.$$

It can be checked that $W_{\mathrm{v}dW}$ is W-like; its two minima of value zero are at $R = R_{\mathrm{v}}$ and $R = R_{\mathrm{l}}$. There are no analytical expressions for R_{v} and R_{l} and

their actual calculation by the use of Equation (11) is somewhat tedious and is not given here. More realistic equations of state have of course the same problem.

If one aims at qualitative results, as we do in this paper, then the numerical awkwardness just pointed out can easily be avoided by postulating a W-function, and naturally choosing the simplest possible form, i.e.,

$$W(R) = (P_c/R_c^4)(R - R_v)^2(R - R_l)^2 \tag{14}$$

(see P1 and P2 where the fluid having such a W-function is called "pseudo-van-der-Waals"). Here P_c and R_c are the pressure and density at the critical point. For this simple model,

$$R_c = (R_v + R_l)/2, \tag{15}$$

while P_c is arbitrary positive. Numerical values for P_c and R_c are not needed because all the equations of the model can be written in dimensionless form and P_c and R_c are absorbed in dimensionless groups. Dimensionless variables are indicated with a tilde overstrike:

$$\tilde{R} = R/R_c, \quad \tilde{R}_v = R_v/R_c, \quad \tilde{R}_l = R_l/R_c, \quad \tilde{W} = W/P_c. \tag{16}$$

Equation (14) becomes

$$\tilde{W}(\tilde{R}) = (\tilde{R} - \tilde{R}_v)^2(\tilde{R} - \tilde{R}_l)^2. \tag{17}$$

The constants $\tilde{R}_v < 1$ and $\tilde{R}_l > 1$ are now parameters that are given as input, instead of being the result of a numerical calculation.

Using this simple W-function in Equation (9), then using (8) we obtain an equation of state. The constant $\bar{M}$ is given by Equation (10) and $\bar{P}$ can be obtained by the condition that the pressure must vanish at zero density. The dimensionless Ψ^b is then

$$\tilde{\Psi}^b(R) = \Psi_b/P_c = (\tilde{R} - \tilde{R}_v)^2(\tilde{R} - \tilde{R}_l)^2 - \tilde{R}_v^2\tilde{R}_l^2. \tag{18}$$

We add for completeness that this free energy function is valid for just one isotherm. It is possible to generalize to arbitrary dimensionless temperatures $\tilde{T}$ (temperature divided by critical temperature) by using

$$\tilde{R}_v = 1 - \sqrt{1 - \tilde{T}}, \quad \tilde{R}_l = 1 + \sqrt{1 - \tilde{T}} \tag{19}$$

(see Equations (90) and (91) in P1; here we have put $\beta = 1$). Substitution of these expressions in Equation (18) leads, after some obvious algebra, to an expression that is valid for all temperatures, even those larger than the critical. There results an equation of state with temperature as a parameter, which has all the characteristics of the van der Waals equation of state (see Appendix A in P1).

We set down here for future reference the expression of fluid viscosity in terms of density that results from using the pseudo van der Waals fluid. Firstly, we easily find the viscosity η_c at critical density by using Equation (15) in Equations (5) and (6):

$$\eta_c = \sqrt{\eta_v \eta_l}. \tag{20}$$

The expression for the dimensionless viscosity, is then

$$\tilde{\eta} = \frac{\eta}{\eta_c} = \left(\frac{\eta_v}{\eta_l}\right)^r, \quad r = \frac{R_l + R_v - 2R}{2(R_l - R_v)}. \tag{21}$$

To summarize: Equation (18) is a simple formula for the Helmholtz free energy per unit volume for bulk fluid, well adapted to qualitative calculations at constant subcritical temperatures. We shall use this formula in this paper, together with formula (21) for viscosity. For quantitative results, the Ψ^b must be obtained through the equation of state, using Equations (9), (10), (11), and (12).

2.3.2. *Wetting and the I-function*

The I-function is a Helmholtz free energy per unit volume introduced in P1 for the description of wetting. It is in general a function of two variables and its determination is not given in P1. However, it is shown in P2 that, if wetting is incomplete at the pore level (i.e., the wetting angle is between 0 and 180°), then I is, to a good approximation, a function of R alone that can be determined in its essential characteristics by the traditional capillary pressure function.

It is easy to show, using Equation (2), that a pressure that can be identified with a capillary pressure exists in the DI-model, and that it is related to the I-function. This can be done by using Equation (7) to write

$$R\nabla(d\Psi/dR) = R\nabla(d\Psi^b/dR) + R\nabla(dI/dR). \tag{22}$$

The first term on the right-hand side can be transformed as follows:

$$R\nabla\frac{d\Psi^b}{dR} = R\frac{d^2\Psi^b}{dR^2}\nabla R = \frac{dP^b}{dR}\nabla R = \nabla P^b,$$

where the second equality comes from taking the derivative of Equation (8), obtaining:

$$\frac{dP^b}{dR} = R\frac{d^2\Psi^b}{dR^2}. \tag{23}$$

The second term on the right-hand side of Equation (22) can be transformed in the same way, i.e.,

$$R\nabla\frac{dI}{dR} = \nabla P^c,$$

by defining a pressure P^c due to wetting by an equation analogous to Equation (23), i.e.,

$$\frac{dP^c}{dR} = R\frac{d^2I}{dR^2}. \tag{24}$$

The velocity, Equation (2) can then be written

$$\mathbf{V} = -\frac{K}{\phi\eta}\left(\nabla(P^b + P^c) + R\nabla G - \Lambda R\nabla\nabla^2 R\right). \tag{25}$$

Note that it is essential for the definition of P^c by the thermodynamical relation (24) that I be a function of R alone. We shall call P^c the capillary pressure function.

We shall now use Equation (24) backwards: we assume that P^c is empirically known and we use the equation to calculate $I(R)$. We assume that $P^c(R)$ is identical with the traditional capillary pressure function $p_c(S)$, provided a conversion from saturation S to density R is used in $p_c(S)$. As we shall see, the identification can only be valid for a limited interval of the density R, implying that I can be constructed from empirical data only inside such a limited interval. Some sort of extrapolation must be done to extend the construction outside the interval.

We show below that I must obey the requirement that $W + I$ must be W-like. See Figure 1a. It follows that its calculation from p_c is the first experimental challenge met by the DI-model.

The argument leading to the requirement on I is as follows. Assume a very long, one-dimensional porous medium in dynamical equilibrium: its velocity is zero everywhere and the variation of density with the space coordinate x is found by solving the differential equation obtained by equating to zero the expression inside the parentheses in Equation (2). Let us assume that $I = 0$ (neutral wetting). The first effect of gravitation, represented by G, is to separate the fluid in a liquid phase (downwards) and

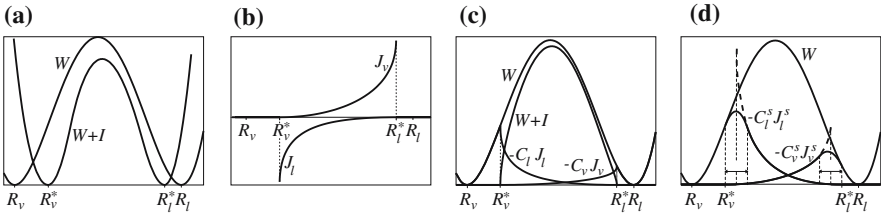

Figure 1. In (a) The W-like functions $W(R)$ and $W(R) + I(R)$. In (b) Functions $J_l(R)$ and $J_v(R)$ defined by Equations (32b) and (33b). In (c) Functions $W(R), -C_v J_v(R), -C_l J_l(R)$, and $W(R) + I(R)$ where $I = C_v J_v + C_l J_l$. In (d) The smoothing of $I(R)$ producing $I^s(R) = C_l^s J_l^s(R) + C_v^s J_v^s(R)$. In (b) and (c), it is assumed that $a_l, a_v < 1$.

a vapor phase (upwards). Gravitation has also the effect of distorting the density profile due to a compression effect downwards. We assume that G is so small that this distortion can be neglected: the density profile at equilibrium is then determined by W and by the boundary conditions specifying that we have liquid at the lower boundary and vapor at the upper boundary. It is then easy to see (the calculation can be done by hand if the simple W of Equation (14) is used) that $R(x)$ is a *smooth* curve, with one plateau where R is equal to R_v, another where R is equal to R_l, and a sigmoid-like curve in between. The smoothness of the curve agrees with observations. Let us now assume mixed wetting so that $I \neq 0$. The equilibrium is now determined by $W + I$ and the only difference with the $I = 0$ case, should be a shift of the two plateaus: the one at R_v is raised at a value R_v^*, the one at R_l is lowered at R_l^*. (We have $R_v < R_v^*$ because of the presence of residual liquid in the pores. Similarly, $R_l > R_l^*$ because of the presence of residual vapor.) The sigmoid must fit *smoothly* to the plateaus to agree with observations; it can have a different shape from the neutral-wetting sigmoid, but that is of secondary importance. Thus $W + I$ must be W-like.

The traditional $p_c(S)$ is an experimentally measured function. We shall use an analytical expression, which depends on four parameters and which covers a large range of measurements (Skjæveland *et al.*, 2000). It is given here with our notation, i.e., with *liquid* and *vapor* as the names of the two phases:

$$p_c(S_l) = C_l \left(\frac{1 - S_{lr}}{S_l - S_{lr}} \right)^{a_l} + C_v \left(\frac{1 - S_{vr}}{1 - S_{vr} - S_l} \right)^{a_v}. \tag{26}$$

S_l is the liquid saturation. The residual liquid saturation S_{lr}, and the residual vapor saturation S_{vr} are considered as input parameters. The constants C_l and C_v are usually referred to as entry pressures and $1/a_l$ and $1/a_v$ as pore size distribution indices. They are here adjustable parameters. The translation from saturation to density is done through Equations (6). We begin by defining R_v^* and R_l^* in terms of input parameters:

$$S_{lr} = \frac{R_v^* - R_v}{R_l - R_v} \iff R_v^* = R_v + (R_l - R_v) S_{lr}, \tag{27a}$$

$$S_{vr} = \frac{R_l - R_l^*}{R_l - R_v} \iff R_l^* = R_l - (R_l - R_v) S_{vr}. \tag{27b}$$

We now identify $P^c(R)$ with $p_c(S_l)$, where S_l is given by Equation (6) (left). For later convenience, we write

$$P^c = P_l^c + P_v^c, \tag{28}$$

where

$$P_{\mathrm{l}}^{\mathrm{c}} = C_{\mathrm{l}} \left(\frac{R_{\mathrm{l}} - R_{\mathrm{v}}^*}{R - R_{\mathrm{v}}^*} \right)^{a_{\mathrm{l}}}, \quad P_{\mathrm{v}}^{\mathrm{c}} = C_{\mathrm{v}} \left(\frac{R_{\mathrm{l}}^* - R_{\mathrm{v}}}{R_{\mathrm{l}}^* - R} \right)^{a_{\mathrm{v}}} \quad (R_{\mathrm{v}}^* < R < R_{\mathrm{l}}^*). \tag{29}$$

Note that P^{c} is only known in the open interval $(R_{\mathrm{v}}^*, R_{\mathrm{l}}^*)$. The boundaries are excluded because the DI-model does not accept infinite pressures.

The integration of Equation (24), using Equation (28), gives

$$I(R) = I_{\mathrm{l}}(R) + I_{\mathrm{v}}(R), \tag{30}$$

with

$$Ia(R) = R \int \frac{P_{\mathrm{a}}^{\mathrm{c}}}{R^2} dR - \alpha_a + \beta_a R \qquad (a = \mathrm{l}, \mathrm{v}), \tag{31}$$

where α_a and β_a are integration constants. We now refer to the second paragraph after the paragraph containing Equation (25): the bounds and constants of integration in Equation (31) must be determined, together with constants C_{l} and C_{v}, in such a way that $W + I$ is a W-like function of R, with two minima at $R = R_{\mathrm{v}}^*$, and $R = R_{\mathrm{l}}^*$, of value zero. It is shown below that this is possible, implying that the model is in agreement with experimental results on capillary pressure. There is a certain reservation to the last statement, as we shall see, relating to the possible infinities in $p_{\mathrm{c}}(S_{\mathrm{l}})$.

We first obtain I_{l} and I_{v} for $R_{\mathrm{v}}^* < \mathrm{R} < R_{\mathrm{l}}^*$.

I_{l} is that part of the I-function which is due to the "liquid-wet part" of the capillary pressure function. We impose the condition that $W + I_{\mathrm{l}}$ should be "as much as possible equal to W" for R in the neighborhood of R_{l}^*:

$$I_{\mathrm{l}}(R_{\mathrm{l}}^*) = 0, \quad I_{\mathrm{l}}'(R_{\mathrm{l}}^*) = 0$$

(where the prime denotes differentiation). Similarly, $W + I_{\mathrm{v}}$ should be "as much as possible equal to W" for R in the neighborhood of R_{v}^*:

$$I_{\mathrm{v}}(R_{\mathrm{v}}^*) = 0, \quad I_{\mathrm{v}}'(R_{\mathrm{v}}^*) = 0.$$

Using these four conditions to determine the constants in Equation (31) with $a = \mathrm{l}$ and with $a = \mathrm{v}$, one easily gets

$$I_{\mathrm{l}}(R) = C_{\mathrm{l}} J_{\mathrm{l}}(R), \tag{32a}$$

$$J_{\mathrm{l}}(R) = \left(\frac{R_{\mathrm{l}} - R_{\mathrm{v}}^*}{R_{\mathrm{l}}^* - R_{\mathrm{v}}^*} \right)^{a_{\mathrm{l}}} \left(1 - \frac{R}{R_{\mathrm{l}}^*} \right) - R \int_R^{R_{\mathrm{l}}^*} \left(\frac{R_{\mathrm{l}} - R_{\mathrm{v}}^*}{R' - R_{\mathrm{v}}^*} \right)^{a_{\mathrm{l}}} \frac{\mathrm{d}R'}{R'^2}, \tag{32b}$$

and

$$I_{\mathrm{v}}(R) = C_{\mathrm{v}} J_{\mathrm{v}}(R), \tag{33a}$$

$$J_{\mathrm{v}}(R) = \left(\frac{R_{\mathrm{l}}^* - R_{\mathrm{v}}}{R_{\mathrm{l}}^* - R_{\mathrm{v}}^*} \right)^{a_{\mathrm{v}}} \left(1 - \frac{R}{R_{\mathrm{v}}^*} \right) + R \int_{R_{\mathrm{v}}^*}^{R} \left(\frac{R_{\mathrm{l}}^* - R_{\mathrm{v}}}{R_{\mathrm{l}}^* - R'} \right)^{a_{\mathrm{v}}} \frac{\mathrm{d}R'}{R'^2}. \tag{33b}$$

It turns out that J_l and J_v are monotonically increasing functions for $R_v^* < R < R_l^*$ (see Figure 1b). There are difficulties connected to the infinity of J_l as $R \to R_v^*$ with $a_l \geq 1$, and to the infinity of J_v as $R \to R_l^*$ with $a_v \geq 1$. We shall temporarily, and for the sake of illustration, assume that the a's are less than 1.

Figure 1b shows J_v and J_l for $a_v = a_l = 0.5$. It is now easy to determine the constants C_l and C_v in such a way that $W + I = 0$ at R_v^* and R_l^*: it suffices to put

$$C_l = -\frac{W(R_v^*)}{J_l(R_v^*)}, \qquad C_v = -\frac{W(R_l^*)}{J_v(R_l^*)}. \tag{34}$$

(It is clear, incidentally, that $C_l > 0$ and that $C_v < 0$.) The resulting $W + I$-function is shown in Figure 1c, together with W, $-C_v J_v$, and $-C_l J_l$. To obtain $I(R)$ outside of the interval $[R_v^*, R_l^*]$ we must now resort to extrapolations. However, $W + I$ must reach the horizontal axis with a horizontal tangent for the extrapolated $W + I$ to be W-like, and it is easy to see from expressions (32b) and (33b) that I, and thus necessarily $W + I$, have vertical tangents at $R = R_v^*$ and $R = R_l^*$. This is due to the infinities of p_c at $S_l = S_{lr}$ and $S_l = 1 - S_{vr}$. The situation is worse when a_l or a_v or both are larger than 1, because then we can not even satisfy $W + I = 0$ at R_v^* and R_l^*.

We make $W + I$ a W-like function by using the fact that the behavior of $p_c(S_l)$, when S_l approaches S_{lr} from above or $1 - S_{vr}$ from below, is not well established (Hassanizadeh and Gray, 1993). Without contradicting experimental evidence we then smooth out the I-function, or rather its two components I_l and I_v, as described below.

There are probably many ways to perform the smoothing. We have chosen to start at the level of the J_l and J_v functions, and to shift their possible infinities away from R_v^* and R_l^*: choosing a small number ϵ, we shift the singularities at $R_v^* + \epsilon$ and $R_l^* - \epsilon$, as shown on Figure 1d. We then define a function J_l^s as follows:

$$J_l^s = \begin{cases} j_l(R), & R_v^* \leq R < R_v^* + 2\epsilon, \\ J_l|_{R_v^* + \epsilon} & R_v^* + 2\epsilon \leq R \leq R_l^*, \end{cases} \tag{35}$$

where $J_l|_{R_v^* + \epsilon}$ is J_l with R_v^* replaced by $R_v^* + \epsilon$. A typical value for ϵ, or rather for its dimensionless counterpart $\tilde{\epsilon} = \epsilon / R_c$ is 0.01. (For the sake of readability, the value of ϵ in Figure 1d is greatly exaggerated.) We choose a second degree polynomial for $j_l(R)$ such that J_l^s and its derivative are continuous at $R = R_v^* + 2\epsilon$: it can then be seen that j_l has just one remaining degree of freedom. A function J_v^s is defined in a similar manner, with a polynomial $j_v(R)$. We now define a smoothed I-function by

$$I^s(R) = C_l^s J_l^s(R) + C_v^s J_v^s(R), \tag{36}$$

and determine the constants $C_{\mathrm{l}}^{\mathrm{s}}, C_{\mathrm{v}}^{\mathrm{s}}$, and the two degrees of freedom in j_{l} and j_{v}, with the four conditions

$$\begin{aligned} &W(R_a^*) + I^{\mathrm{s}}(R_a^*) = 0 \\ &W'(R_a^*) + I^{\mathrm{s}\prime}(R_a^*) = 0 \end{aligned} \quad (a = \mathrm{l}, \mathrm{v})$$

(the primes denote differentiation). The calculations are elementary but somewhat long and are not given here. It is to be noted that the C's appearing in the capillary pressure correlation are not free parameters, according to the DI-model.

We now look at the problem of extending the I^{s}-function, to the left of R_{v}^* and to the right of R_{l}^*. We denote this function by I^{se}. The extension is done as follows. To the left of R_{v}^* we take $W + I^{\mathrm{se}}$ to be equal to W, translated by the amount $R_{\mathrm{v}}^* - R_{\mathrm{v}}$: this is the vapor phase region and we expect it to behave approximately as a pure vapor. To the right of R_{l}^* we want the liquid to behave as a nearly incompressible fluid and we impose therefore that

$$W(R) + I^{\mathrm{se}}(R) = \frac{P_{\mathrm{c}}}{R_{\mathrm{c}}^2} \frac{(R - R_{\mathrm{l}}^*)^2}{4\tilde{\epsilon}},$$

where $\tilde{\epsilon}$ is the small parameter used previously. The function $W(R) + I^{\mathrm{se}}(R)$ is shown in Figure 1 as the curve labeled $W + I$.

To summarize: Function $I^{\mathrm{se}}(R)$ is calculated from the empirical capillary pressure function and the equation of state on an interval $[R_{\mathrm{v}}^* + 2\epsilon, R_{\mathrm{l}}^* - 2\epsilon]$ which excludes the possible infinities of the capillary pressure function. Outside this interval it is extrapolated as simply as possible, keeping in mind that $W + I$ must be W-like.

2.4. THE MODEL IN SUMMARY

The model consists of: (i) the flow equation (1), (ii) an initial condition on the fluid density R, and (iii) boundary conditions of type (d) or (e) (see Equations (4b)). There are two input functions: the fluid viscosity $\eta(R)$ (see Section 2.2) and the total Helmholtz free energy per unit volume of bulk fluid $\Psi(R)$ (see Section 2.3).

The input parameters are as follows. Firstly the permeability K, the porosity ϕ, a constant characterizing gravity (usually the acceleration g), and Λ. The last mentioned is related to the thickness of the transition region as shown in P1 and P2. Secondly, the constants inherent to the functions η and Ψ. The former has a minimum of two parameters, namely the viscosities η_{v} and η_{l} of the pure phases. The latter has a minimum of six parameters: the densities R_{v} and R_{l} of the pure phases, the residual saturations S_{vr} and S_{lr}, and the two a's of the capillary pressure correlation (Equation (26)).

3. Analytical Relative Permeabilities for Stabilized Flows

The formulas defining relative permeabilities can be turned into analytic expressions if the flow can be characterized as a constant velocity traveling wave. See P2 where these formulas were restricted to the case of a vapor wet rock. We shall here generalize them to the case of a mixed wet rock.

We need the derivative of the capillary pressure with respect to R. The smoothing and continuation of the I-function performed in Section 2.3.2 implies that we must use the derivative of a function P^{cs} (a smoothed and continued P^{c}). Using the earlier splitting up into a liquid and a vapor wetting part (Equation (28)), we introduce

$$\frac{dP^{\mathrm{cs}}}{dR} = \frac{dP_{\mathrm{l}}^{\mathrm{cs}}}{dR} + \frac{dP_{\mathrm{v}}^{\mathrm{cs}}}{dR}, \tag{37}$$

with

$$\frac{dP_{\mathrm{l}}^{\mathrm{cs}}}{dR} = R\frac{d^2}{dR^2}C_{\mathrm{l}}^{\mathrm{s}}J_{\mathrm{l}}^{\mathrm{s}}(R), \quad \frac{dP_{\mathrm{v}}^{\mathrm{cs}}}{dR} = R\frac{d^2}{dR^2}C_{\mathrm{v}}^{\mathrm{s}}J_{\mathrm{v}}^{\mathrm{s}}(R) \tag{38}$$

(see Equations (24) and (36)).

The relative permeabilities (k_{rl} and k_{rv} for the liquid and vapor phases) can now be given the same form as in P2, namely

$$k_{\mathrm{rl}} = \frac{S_{\mathrm{l}}^*}{1+(R_{\mathrm{v}}^*/R_{\mathrm{l}}^*)\gamma(S_{\mathrm{l}}^*)}, \tag{39a}$$

$$k_{\mathrm{rv}} = \frac{1-S_{\mathrm{l}}^*}{1+\gamma(1-S_{\mathrm{l}}^*)}, \tag{39b}$$

where

$$S_{\mathrm{l}}^* = \frac{\tilde{R}-\tilde{R}_{\mathrm{v}}^*}{\tilde{R}_{\mathrm{l}}^*-\tilde{R}_{\mathrm{v}}^*}. \tag{40}$$

The generalization to the mixed wet case proceeds from the following straightforward generalization of the function γ given by Equation (61) of P2:

$$\gamma(S_{\mathrm{l}}^*) = -\left[\frac{1}{\tilde{g}\tilde{R}_{\mathrm{v}}^*}\frac{d\tilde{P}_{\mathrm{v}}^{\mathrm{cs}}}{d\tilde{R}}\sqrt{\frac{2}{\tilde{\Lambda}}[\tilde{W}(\tilde{R})+\tilde{I}^{\mathrm{s}}(\tilde{R})]}\right]_{\tilde{R}=\tilde{R}_{\mathrm{l}}^*-(\tilde{R}_{\mathrm{l}}^*\tilde{R}_{\mathrm{v}}^*)S_{\mathrm{l}}^*} - \\ -\left[\frac{1}{\tilde{g}\tilde{R}_{\mathrm{v}}^*}\frac{d\tilde{P}_{\mathrm{l}}^{\mathrm{cs}}}{d\tilde{R}}\sqrt{\frac{2}{\tilde{\Lambda}}[\tilde{W}(\tilde{R})+\tilde{I}^{\mathrm{s}}(\tilde{R})]}\right]_{\tilde{R}=\tilde{R}_{\mathrm{v}}^*+(\tilde{R}_{\mathrm{l}}^*-\tilde{R}_{\mathrm{v}}^*)S_{\mathrm{l}}^*}, \tag{41}$$

where the quantities with tildes are dimensionless. Densities ($\tilde{R}, \tilde{R}^*_v$) are referred to R_c, pressures ($\tilde{P}^{cs}_v, \tilde{P}^{cs}_l$) and potentials ($\tilde{W}, \tilde{I}^s$) are referred to P_c, and

$$\tilde{g} = (R_c L / P_c) g, \quad \tilde{\Lambda} = (R_c^2 / (P_c L^2)) \Lambda, \tag{42}$$

where L is the length of the porous medium along which the wave is traveling.

It can be shown that, if a_v and a_l in Equation (26) are both less that 1, then the smoothing of the I-function is not necessary for the calculation of the relative permeabilities. The superscript s can be dropped in Equation (41): Equation (29) can be used to calculate the derivatives of $\tilde{P}^c_l$ and $\tilde{P}^c_v$, and one can use the I-function defined by Equations (30), (32a), (33a), and (34).

Thus knowledge of the equation of state, of the capillary pressure, of the parameters belonging to these functions, and of the constants g and Λ, lead to the calculation of the relative permeabilities for stabilized flows.

4. A Numerical Application

In this section we apply the DI-model presented above to a numerical investigation of relative permeabilities for non-stabilized flows. We force the flows to be nonstabilized by the use of start and boundary conditions. We begin with an outline of a method for calculating relative permeabilities numerically.

4.1. "EXPERIMENTAL" RELATIVE PERMEABILITIES

We assume a one-dimensional porous medium of length L, mixed wetting, and we begin with the definition of relative permeabilities:

$$\tilde{V}^*_l = \frac{k_{rl(exp)}}{\tilde{\eta}(\tilde{R}^*_l)} \left(-\frac{\partial \tilde{p}^*_l}{\partial \tilde{x}} + \tilde{g} \tilde{R}^*_l \right), \quad \tilde{V}^*_v = \frac{k_{rv(exp)}}{\tilde{\eta}(\tilde{R}^*_v)} \left(-\frac{\partial \tilde{p}^*_v}{\partial \tilde{x}} + \tilde{g} \tilde{R}^*_v \right). \tag{43}$$

The dimensionless quantities not already defined are as follows: $\tilde{x} = x/L$, and x is the coordinate which increases in the direction of the force of gravity; $\tilde{p}^*_l$ and $\tilde{p}^*_v$ are pressures, referred to P_c as earlier in the paper. The velocities on the left-hand sides are made dimensionless by the following general formula, valid for all other velocities used later in the paper:

$$\tilde{V} = (\phi \eta_c L / (K P_c)) V. \tag{44}$$

The DI-model does not provide phase velocities, nor any other phase quantities. To obtain them we generalize the method used in P2. We begin with

the dimensionless velocity $\tilde{V}$ and momentum $\tilde{\Gamma}$, defined as follows:

$$\tilde{V} = -\frac{\tilde{R}}{\tilde{\eta}(\tilde{R})}\frac{\partial}{\partial \tilde{x}}\left(\frac{d\tilde{\Psi}}{d\tilde{R}} - \tilde{g}\tilde{x} - \tilde{\Lambda}\frac{\partial^2 \tilde{R}}{\partial \tilde{x}^2}\right), \quad \tilde{\Gamma} = \tilde{R}\tilde{V}. \tag{45}$$

We now introduce the following notation for the velocities and momenta at, respectively, $S_1^* = 0$ and $S_1^* = 1$:

$$\begin{aligned} &\tilde{V}_0 = \tilde{V}|_{S_1^*=0}, \quad \tilde{V}_1 = \tilde{V}|_{S_1^*=1}, \\ &\tilde{\Gamma}_0 = \tilde{\Gamma}|_{S_1^*=0}, \quad \tilde{\Gamma}_1 = \tilde{\Gamma}|_{S_1^*=1}. \end{aligned} \tag{46}$$

Following P2 we then postulate that

$$\tilde{V}_1^* = \frac{\tilde{\Gamma}_0 - \tilde{\Gamma}}{\tilde{\Gamma}_0 - \tilde{\Gamma}_1}\tilde{V}_1, \quad \tilde{V}_v^* = \frac{\tilde{\Gamma} - \tilde{\Gamma}_1}{\tilde{\Gamma}_0 - \tilde{\Gamma}_1}\tilde{V}_0. \tag{47}$$

As pointed out in P2, these equations ensure that the local momenta carried by each phase add to the total fluid momentum. We can, with Equation (47), obtain the phase velocities during the calculation of a given process, since all quantities on the right-hand sides are calculable.

Turning to the pressure gradients in the two phases, the central argument leading to their calculation is given in P2 as follows. If $\tilde{P}^b$ denotes the bulk pressure in the fluid, then the gradient of $\tilde{P}^b$ is zero *at equilibrium and when wetting is absent* since, following the Maxwell construction, the van der Waals "loops" in the equation of state are replaced by an horizontal line. With wetting, where the $\tilde{W}$-function is replaced by $\tilde{W} + \tilde{I}^s$, it is the gradient of $\tilde{P}^b + \tilde{P}^{cs}$ that must vanish at equilibrium. It follows that

$$\left[\frac{\partial \tilde{P}^b}{\partial \tilde{x}}\right]_{eq} = -\frac{\partial \tilde{P}^{cs}}{\partial \tilde{x}} = -\frac{d\,\tilde{P}^{cs}}{d\tilde{R}}\frac{\partial \tilde{R}}{\partial \tilde{x}}. \tag{48}$$

For the simple case of a vapor wetting medium considered in P2, one identifies the pressure gradient in each phase with the left-hand side of Equation (48), taken at the proper value of the saturation. Generalizing to mixed wetting, we put

$$\frac{\partial \tilde{p}_l^*}{\partial \tilde{x}} = -\tilde{g}\tilde{R}_v^*\gamma_{exp}(S_l^*), \quad \frac{\partial \tilde{p}_v^*}{\partial \tilde{x}} = -\tilde{g}\tilde{R}_v^*\gamma_{exp}(1 - S_l^*). \tag{49}$$

where γ_{exp} is

$$\gamma_{exp}(S_l^*) = -\left[\frac{1}{\tilde{g}\tilde{R}_v^*}\frac{d\tilde{P}_v^{cs}}{d\tilde{R}}\left|\frac{\partial \tilde{R}}{\partial \tilde{x}}\right|\right]_{1-S_l^*} - \left[\frac{1}{\tilde{g}\tilde{R}_v^*}\frac{d\tilde{P}_l^{cs}}{d\tilde{R}}\left|\frac{\partial \tilde{R}}{\partial \tilde{x}}\right|\right]_{S_l^*}. \tag{50}$$

In this expression, the derivatives of $\tilde{P}_l^{cs}$ and $\tilde{P}_v^{cs}$ are given by Equation (38), while the partial derivative of $\tilde{R}$ is obtained by using the solution of

the partial differential equations. (In stabilized flow, an analytical expression can be found for this partial derivative, leading to the expressions of Section 3.)

One can thus calculate

$$k_{\mathrm{rl(exp)}} = \frac{\tilde{V}_{\mathrm{l}}^* \tilde{\eta}(\tilde{R}_{\mathrm{l}}^*)}{\tilde{g}\tilde{R}_{\mathrm{l}}^*} \frac{1}{1 + (R_{\mathrm{v}}^*/R_{\mathrm{l}}^*)\gamma_{\mathrm{exp}}(S_{\mathrm{l}}^*)}, \tag{51a}$$

$$k_{\mathrm{rv(exp)}} = \frac{\tilde{V}_{\mathrm{v}}^* \tilde{\eta}(\tilde{R}_{\mathrm{v}}^*)}{\tilde{g}\tilde{R}_{\mathrm{v}}^*} \frac{1}{1 + \gamma_{\mathrm{exp}}(1 - S_{\mathrm{l}}^*)}, \tag{51b}$$

at any time step and at values of $\tilde{x}$ where the density $\tilde{R}$ is intermediate between $\tilde{R}_{\mathrm{v}}^*$ and $\tilde{R}_{\mathrm{l}}^*$.

4.2. NUMERICAL EXPERIMENTS

We have done three numerical experiments, where one can be characterized as a drainage, and two as imbibitions. We have labeled them Drainage, Imbibition 1, and Imbibition 2: see Appendix A for the parameter specifications, and for the initial and boundary conditions. In the "Drainage" and "Imbibition 1" cases the boundary conditions have been determined in such a way that flow velocities decrease and static final states are approached, with both phases clearly present. In the "Imbibition 2" case the boundary conditions do not allow a static final state to occur before most of the medium is filled with liquid.

The results of the drainage calculation are shown in Figure 2. The solution $\tilde{R}(\tilde{x}, \tilde{t})$ of the flow Equation (1) is shown in (a). Note the qualitative agreement with the experimental results of Terwilliger *et al.* (1951) (see in particular their Figure 2). Parts (b) and (c) are plots of the liquid and vapor velocities (Equation (47)), versus the normalized liquid saturation (Equation (40)). The essential information contained in Figures (b) and (c) is that we have counter-current flow: liquid velocity is positive so that the liquid phase moves in the direction of the gravitational force, while the vapor phase moves in the opposite direction. In other words, the liquid falls, leaving a rising vapor behind it.

Similar figures for the imbibition calculations are not shown here. The main features are as follows.

For Imbibition 1 we again have counter-current flow, with the liquid phase being drawn upwards, against the gravitational force, while the vapor phase falls into the rising liquid and liquefies. The inter-phase region (i.e., the diffuse interface) rises and liquid is drawn in the medium from below thus justifying the name "imbibition". The only non-conventional feature is the gas being drawn in the medium from above and liquefying.

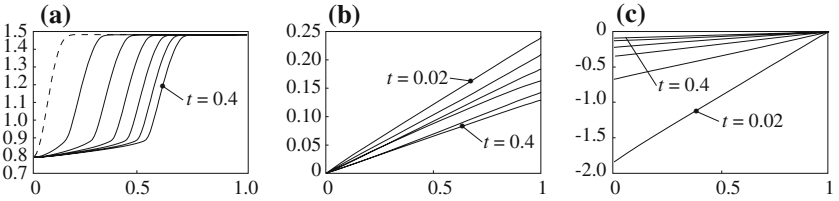

Figure 2. Drainage simulation. In (a) Fluid density versus $\tilde{x}$, given by the solution of Equation (1) with the specifications given in Appendix A, for $\tilde{t}$-values of 0, 0.02, 0.08, 0.16, 0.32, 0.40 (increasing from the broken line and to the right). In (b) Dimensionless liquid velocity versus normalized liquid saturation S_l^*, for $\tilde{t}$-values of 0.02, 0.08, 0.16, 0.32, 0.40, increasing from top to bottom as indicated. In (c) Dimensionless vapor velocity versus normalized liquid saturation S_l^*, for the same $\tilde{t}$-values as in (b), increasing from bottom to top as indicated.

The physics is somewhat more complex for Imbibition 2: flow is now co-current, both phases moving with positive velocities, i.e., in the direction of the gravitational force. But the vapor velocity is about ten times larger than the liquid velocity so that we have the same overall effect as in Imbibition 1, i.e., vapor falling into liquid and liquefying. The inter-phase region rises, but liquid is expelled from below and vapor is drawn in from above. Thus we do not have imbibition in the traditional sense, but we have kept the name since the overall liquid saturation in the medium increases and the "interface" rises.

4.3. DISCUSSION OF THE RESULTS OF THE NUMERICAL EXPERIMENTS

"Experimental" relative permeabilities are calculated for each of the three processes presented in Section 4.2, and for a number of $\tilde{t}$-values between 0 and 0.4. The results of these calculations are shown on Figure 3, top row.

We first take up the fact, apparent from the figure, that the model predicts relative permeabilities larger than one. The explanation is found in the expression for fluid velocity, Equation (2). In one spatial dimension and using the thermodynamical relations of Section 2.3, one finds

$$V = -\frac{K}{\phi\eta}\left(\frac{\partial P^{\mathrm{b}}}{\partial x} - gR\right) - \frac{KR}{\phi\eta}\left(\frac{d^2 I}{dR^2}\frac{\partial R}{\partial x} - \Lambda\frac{\partial^3 R}{\partial x^3}\right). \tag{52}$$

We shall refer to the first and second terms on the right-hand side as the Darcy and DI-non-Darcy (not to be confused with the inertial non-Darcy velocity) velocities. Obviously, the calculations of relative permeabilities are a two step process where the first step is to partition the fluid velocity in its liquid and vapor parts. The second step consist essentially in taking away the DI-non-Darcy term and accounting for its contribution by a factor (the relative permeability) multiplying the Darcy term.

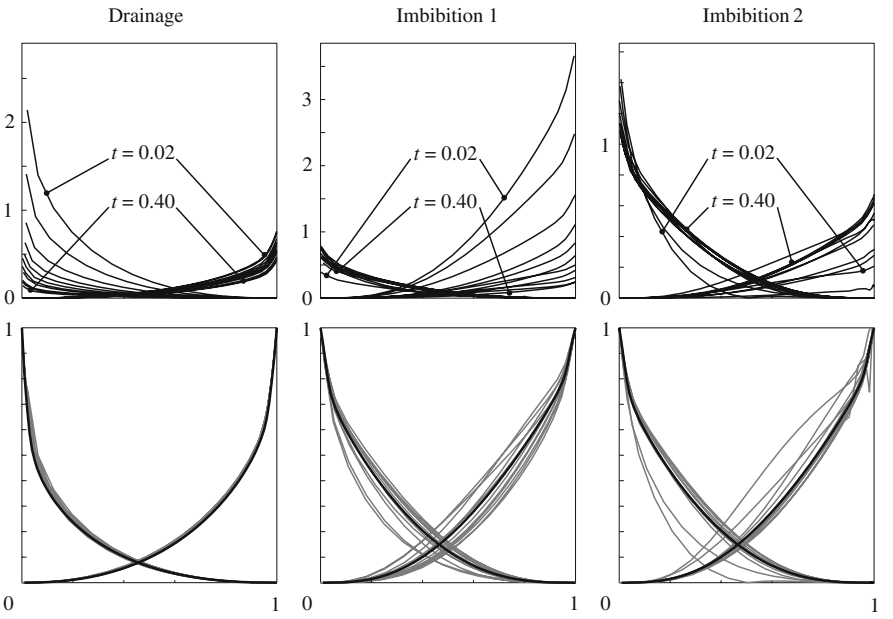

Figure 3. Liquid (ascending curves) and vapor (descending curves) relative permeabilities versus normalized liquid saturation S_l^*, for the three processes specified in Appendix A and for $\tilde{t}$-values of 0.02, 0.04, then up to 0.40 by steps of 0.04. Top row: calculated, see Equation (51). Bottom row: drawn in gray are the curves of the top row, with ordinates divided by their (largest) end-point values; drawn in black are the theoretical relative permeabilities of Section 3.

One important difference between stabilized flow types considered in P2 and the non-stabilized ones considered here is illustrated in Figure 4. For stabilized flow types (left) the large gradients in the density are confined to the transition region so that the DI-non-Darcy term only contributes to the velocity inside that region. This contribution gradually vanishes as one approaches the 100% liquid or vapor regions, which leads to a relative permeability that behaves as expected, being in particular less than 1. For non-stabilized flow types (right) the large gradients show a tendency to spill over in the 100% liquid and vapor regions, so that the DI-non-Darcy term remains important in the pure-phase regions, giving a velocity that is larger than what is expected from the Darcy expression. Accounting for the non-Darcy term by a multiplicative factor leads in this case to the factor being larger than 1.

The question that immediately arises is whether permeabilities larger than 1 are experimentally observable. To answer this question we note that the very large relative permeabilities occur for small times, and for the phase for which the dimensionless velocities are roughly larger than 1: see Figures 2 and 3. The reference velocity (see Equation (44)) is $K P_c/(\phi \eta_c L)$.

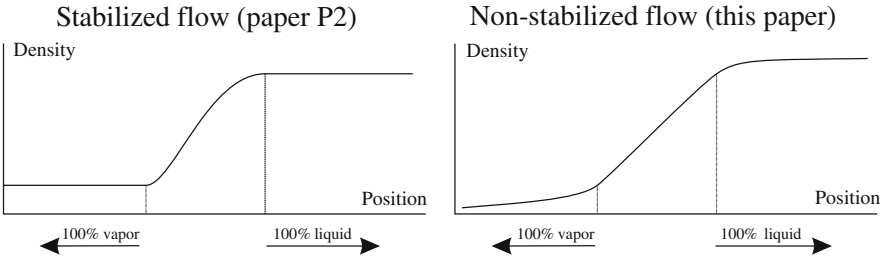

Figure 4. In stabilized flow types the large gradients are confined to the transition region.

Using the following laboratory values

$$K = 100\,\text{mD} \qquad \phi = 0.3 \qquad L = 20\,\text{cm}$$
$$P_c = 2.21 \times 10^7\,\text{N/m}^2, \quad \eta_c = 0.042\,\text{cP}$$

(where critical pressure P_c and critical viscosity η_c belong to the water–steam system) we get a reference velocity of the order of 1 m/s. This is at least 10,000 times larger than the usually occurring velocities, which explains that relative permeabilities larger than one are not observed.

The other obvious feature of the top row of Figure 3 is the absence of a unique relative permeability curve. The present model thus confirms the well-accepted fact that relative permeabilities are not functions of saturation alone. In fact, the foregoing discussion has shown that the relative permeabilities are linked to the second term on the right-hand side of Equation (52), i.e., to the density and its derivatives. In view of our simple relation (Equations (6)) between density and saturation, a reasonable assumption would be that

$$k_{ra} = k_{ra}(S, \partial S; P) \quad (a = 1, v).$$

Here we have used ∂S is a shorthand notation for the dependence of k_{ra} on the partial derivatives of S of (in principle) all orders; P stands for a set of parameters which usually do not vary with time and space, like pure phase densities, viscosities, and other parameters included in the definition of the equation of state, and the capillary pressure.

The bottom row of the Figure 3 is a redrawing of the curves of the top row, after a renormalization consisting in dividing the ordinates of each curve by the curve's end-point ordinate (left end point for the vapor, right end point for the liquid relative permeabilities). The analytical curves of Section 3 are also drawn. A gathering of the renormalized curves, like the one happening for the Drainage case, would have indicated that relative permeabilities are functions of the type $f(S; P)g(\partial S; P)$. Obviously, the DI-model clearly indicates that such simplified functional dependence does not exist in general.

5. Conclusions

We have presented the DI-model of two-phase flow in porous media. This paper clarifies questions left open in two previous papers (referred to above as P1 and P2), concerning the description of wetting. In particular, it elaborates on the assumption of incomplete wetting at the pore level, introduced in P2.

The main limitation of the model is in its assumption of one chemical component, which restricts its applicability to liquid–vapor systems, or to systems whose thermodynamical description can be approximated by that of a liquid–vapor system.

The advantage of the model is a theoretical description which incorporates the separation of the phases as an integral part of the solution of the flow equation. Thus numerical dispersion, with spurious breakthroughs of a mobile phase, does not occur. The absence of relative permeabilities is an additional advantage.

Concerning capillary pressure: a function $P^{\mathrm{c}}(R)$ has been defined, not as the difference $P^{\mathrm{n}} - P^{\mathrm{w}}$ between the pressures in the non-wetting and the wetting phases, but as a quantity with the formal properties of a pressure. The P^{c}-function is related to that part of the Helmholtz free energy per unit volume (the I-function) which pertains to the description of wetting, in the same formal manner as the bulk pressure P^{b} is related to Ψ^{b}: see Equations (23) and (24). It is then natural to identify $P^{\mathrm{c}}(R)$ with the traditional capillary pressure function $p_{\mathrm{c}}(S)$, with the purpose of calculating the I-function, provided a definition of saturation as a function of density is given, and provided one keeps in mind that this identification does not yield $I(R)$ for all R. (See Section 2.3.2.) Some statements about $p_{\mathrm{c}}(S)$ resulting from this identification are as follows: (i) p_{c} is not, in general, a function of state, in the thermodynamic sense (see P1); (ii) p_{c} is, to a good approximation, a function of state if one assumes incomplete wetting, i.e., wetting angles strictly between 0 and 180°, at the pore level, or if one assumes permeabilities of the order of one Darcy and above (see P2); (iii) p_{c} can not become infinite. It is to be noted that similar statements have been made in Hassanizadeh and Gray (1993): see their comments in connection with their Equations (14), (15), and (44).

Concerning relative permeabilities: the DI-model does not use them but it can, assuming its experimental correctness, be used to perform simulations leading to their evaluation. The conclusions from such simulations are as follows. Analytical expressions exist (see Section 3) and can be used for *constant velocity traveling wave* flow types. For other flow types, the model confirms the belief that relative permeabilities, as functions of saturation alone, cannot capture the full complexity of two-phase flow. In fact, the model indicates a likely dependence on the *spatial derivatives* of the

saturation. In addition, the model does not confirm the hypothesis of a separation of the functional dependence on saturation from the functional dependence on derivatives of saturation.

Concerning experimental verification: *qualitative* verification results first from the fact that I can be calculated from p_c (after adjusting its commonly assumed infinities) in such a way that $W + I$ is W-like. We would also like to point out the resemblance of the drainage curves of Figure 2 with the classical results of Terwilliger *et al.* (1951). *Quantitative* verification with published results is, for the time being, not feasible since the information on thermodynamical properties, which is necessary for the simulations with the DI-model is usually not provided.

Appendix. Specifications for the Numerical Experiments of Section 4.2

The flow equation in one dimension, with the space axis pointing in the direction of the gravitational force (downwards), is

$$\frac{\partial \tilde{R}}{\partial \tilde{t}} = \frac{\partial}{\partial \tilde{x}} \left[\frac{\tilde{R}^2}{\tilde{\eta}(\tilde{R})} \frac{\partial}{\partial \tilde{x}} \left(\frac{d\tilde{\Psi}}{d\tilde{R}} - \tilde{\Lambda} \frac{\partial^2 \tilde{R}}{\partial \tilde{x}^2} - \tilde{g}\tilde{x} \right) \right],$$

using dimensionless quantities defined in the main text and with

$$\tilde{t} = (K P_c/(\phi \eta_c L^2))t.$$

We have chosen

$$\tilde{\Lambda} = 0.01, \quad \tilde{g} = 0.5, \quad \eta_v/\eta_l = 0.1.$$

We have used the pseudo-van-der-Waals fluid, i.e., the fluid having the $\tilde{\Psi}^b$ given by Equation (18). The parameters describing this function and the $\tilde{I}$-function of Section 2.3.2 are chosen as follows:

$$\begin{array}{llll} \tilde{R}_l = 1.6, & \tilde{R}_v = 0.4, & S_{lr} = 0.4, & S_{vr} = 0.1, \\ a_l = 0.50, & a_v = 1.15, & \text{for drainage,} & \\ a_l = 1.00, & a_v = 1.40, & \text{for imbibition.} & \end{array} \tag{A.1}$$

The numerical values on the first line imply that the minima of the W-function are at $\tilde{R}_v^* = 0.88$ (density of phase consisting of pure vapor and residual liquid) and $\tilde{R}_l^* = 1.48$ (density of phase consisting of pure liquid and residual vapor). Note the different choices for a_l and a_v, depending on whether one simulates drainage or imbibition. The two resulting capillary pressure functions, given by Equation (26), are shown in Figure A.1 (see Section 2.3.2 for the calculation of C_l and C_v or rather of C_l^s and C_v^s.).

The initial conditions are as follows: $\tilde{R}(\tilde{x}, 0)$ is first given by a step function, where $\tilde{R} = \tilde{R}_v^*$ for $\tilde{x}$ less than the position of the discontinuity, and

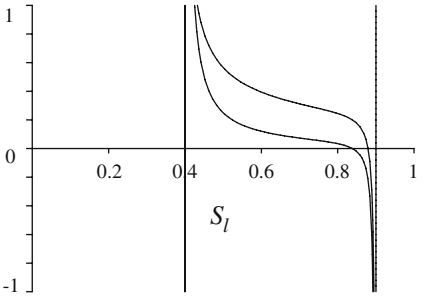

Figure A.1. The capillary pressure functions versus liquid saturation S_l, resulting from constants given in (A.1), see Equation (26). (The left vertical asymptote is at $S_l = S_{lr}$, the right one at $S_l = 1 - S_{vr}$.) The upper curve is used for drainage, the lower for imbibition simulations.

$\tilde{R} = \tilde{R}_1^*$ otherwise. The position of the discontinuity is at about 0.1 for drainage, at about 0.9 for imbibition. The step function is then smoothed (see the broken line in Figure 2a).

The boundary conditions are of the type (d) (see Equation (4b)), i.e., $\tilde{R}(\tilde{x}, \tilde{t})$ and $\tilde{R}_x(\tilde{x}, \tilde{t})$ (the partial derivative of R with respect to x) are given for all $\tilde{t}$ at $\tilde{x} = 0$ and $\tilde{x} = 1$:

$$\begin{aligned} &\tilde{R}(0, \tilde{t}) = \tilde{R}_0, \quad \tilde{R}_x(0, \tilde{t}) = 0, \\ &\tilde{R}(1, \tilde{t}) = \tilde{R}_1, \quad \tilde{R}_x(0, \tilde{t}) = 0. \end{aligned} \tag{A.2}$$

The values of $\tilde{R}_0$ and $\tilde{R}_1$ depend on the simulated process and are as follows:

$$\begin{aligned} &\text{Drainage:} \quad \tilde{R}_0 = 0.7902 \quad \tilde{R}_1 = 1.4824 \\ &\text{Imbibition 1:} \quad \tilde{R}_0 = 0.8427 \quad \tilde{R}_1 = 1.4866 \\ &\text{Imbibition 2:} \quad \tilde{R}_0 = 0.8800 \quad \tilde{R}_1 = 1.4800. \end{aligned} \tag{A.3}$$

References

Anderson, D. M., McFadden, G. B. and Wheeler, A. A.: 1998, Diffuse-interface methods in fluid mechanics, *Ann. Rev. Fluid. Mech.* **30**, 139–165.

Hassanizadeh, S. M. and Gray, W. G.: 1993, Thermodynamic basis of capillary pressure in porous media, *Water Resour. Res.* **29**, 3389–3405.

Marle, C. M.: 1982, On macroscopic equations governing multiphase flow with diffusion and chemical reactions in porous media, *Int. J. Eng. Sci.* **20**, 643–662.

Novick-Cohen, A. and Segel, L. A.: 1984, Non-linear aspects of the Cahn–Hilliard equation, *Physica D* **10**, 277–298.

Papatzacos, P.: 2000, Diffuse-interface models for two-phase flow, *Phys. Scripta* **61**, 349–360.

Papatzacos, P.: 2002, Macroscopic two-phase flow in porous media assuming the diffuse-interface model at pore level, *Transport Porous Media* **49**, 139–174.

Papatzacos, P. and Skjæveland, S. M.: 2004, Relative permeability from thermodynamics, *SPE J.* (March 2004), 47–56.

Skjæveland, S. M., Siqveland, L. M., Hammervold, W. L. and Virnovsky, G. A.: 2000, Capillary pressure correlation for mixed-wet reservoirs. *SPEREE* (February 2000), 60–67.

Terwilliger, P. L., Wilsey, L. E., Hall, H. N., Bridges, P. M. and Morse, R. A.: 1951, An experimental and theoretical investigation of gravity drainage performance, *Trans.* AIME **192**, 285–296.